Progress In Electromagnetics Research Letters, Vol. 101, 49–54, 2021

Spur-Less Interdigital Metal-Insulator-Metal Capacitor

Na Xie, Huanyan Tie, Qiang Ma, and Bo Zhou*

Abstract—A wideband interdigital metal-insulator-metal (MIM) capacitor is created and built in a two-layer low temperature co-fired ceramic (LTCC) substrate. To reduce the number of stopbands and eliminate unexpected spurs which restrict the bandwidth, short-interconnection that interconnects the open ends of interval fingers is proposed. The increment of bandwidth and capacitance of the proposed interdigital MIM capacitor is 206% and 25%, respectively. The proposed interdigital capacitor has a wider frequency applicational range and a compact size of only 8.2×6.2 mm. Performance discussion and comparisons are also carried out.

1. INTRODUCTION

Metal-insulator-metal (MIM) capacitors are widely used in microwave integrated circuits (MICs) and systems design with its advantages of simple structure, compact size, and comparative large capacitance [1]. For a greater capacitance, the vertically placed upper and lower plates of MIM capacitor are designed in an interdigital form with more fingers. The conventional interdigital MIM capacitor structure, planar view, equivalent circuit, and corresponding typical s-parameters are shown in Figures 1(a), (b), (c), and (d), respectively. In Figure 1(d), the unexpected spurs at frequencies f_1, f_2, f_3, f_4, and f_5 can be noticed. Bond wire interconnections and via transitions have been adopted to remove the unexpected spurs of planar interdigital capacitors and vertically-interdigital-capacitors (VICs) [2–6]; however, the spur elimination for interdigital MIM capacitors has not been reported yet.

In this paper, an interdigital MIM capacitor is created with the purpose of enhancing working frequency and equivalent capacitance. The neoteric creation is that the added short-interconnections of interval fingers help to cut down the number of stopbands. Not only did the bandwidth enhance 206%, but also the capacitance enhanced 25% after comparing with traditional equivalent implementation. The creation is presented with both numerical analysis and test experiment.

2. CIRCUIT DESIGN AND ANALYSIS

Shown in Figure 1(c), 14 inductor and capacitor elements in series or parallel interconnection forms establish stopband structures, which produce the undesired spurs. As long as the number of stopband structures is lowered, the undesired spurs can vanish. The proposed interdigital MIM capacitor with 8 fingers is created and built on a 2-layer LTCC substrate. The even-fingers take up the 1^{st}-layer; the odd-fingers take up the 2^{nd}-layer; and the bottom layer is the ground layer. The 3D structure and planar view of the proposed interdigital MIM capacitor are revealed in Figures 2(a) and (b), respectively. The odd-number fingers' open ends are short-interconnected with a strip-line on Layer 2, and the even-number fingers' open ends are interconnected with a microstrip line on Layer 1. Figures 2(c), (d), and (e) show the equivalent circuit after adding short-interconnections, equivalent circuit after regrouping LC

Received 1 October 2021, Accepted 27 November 2021, Scheduled 2 December 2021

* Corresponding author: Bo Zhou (sarahxboy@hotmail.com).

The authors are with the College of Electronic and Optical Engineering, Nanjing University of Posts and Telecommunications, Nanjing, China.

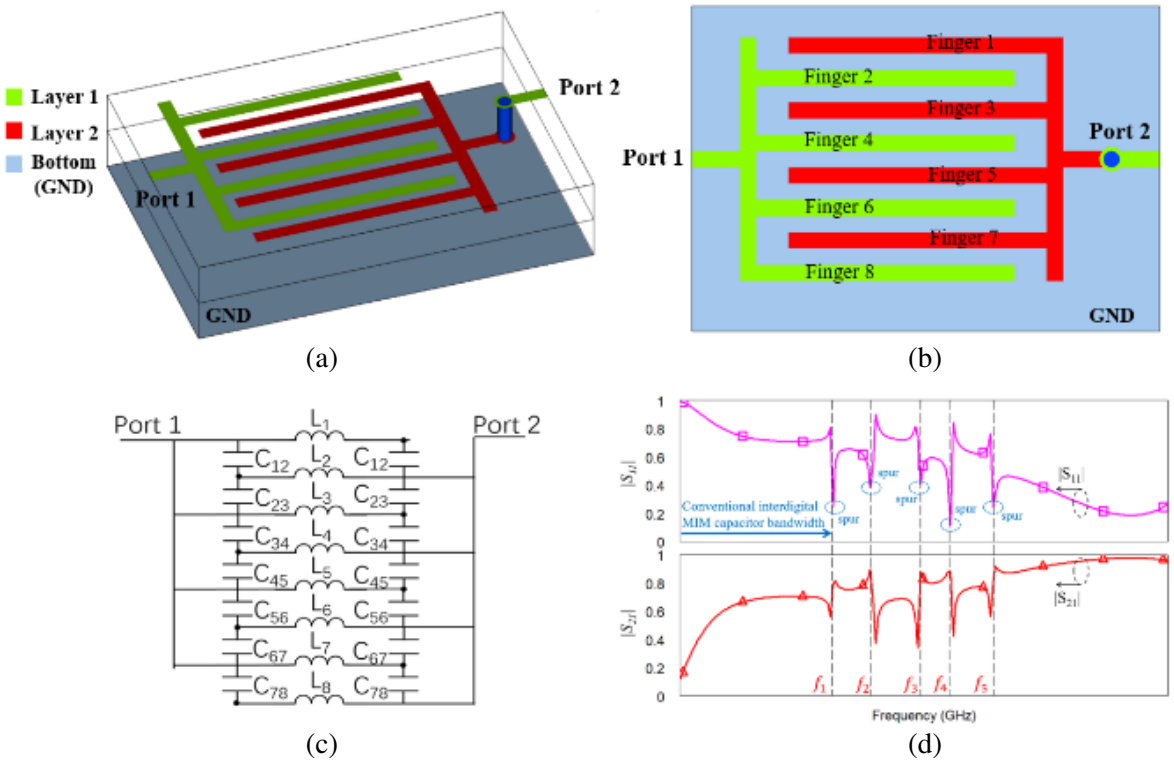

Figure 1. Conventional interdigital MIM capacitor, (a) 3D structure, (b) planar view, (c) equivalent circuit and (d) corresponding s-parameters with unwanted spurs.

elements, and final equivalent circuit, respectively. Adopting the short-interconnection transmission line to short-connect interconnect the alternate fingers can help to reduce the quantity of stopbands, and the process can be illustrated in Figures 2(c), (d), and (e). 14 series inductors L_n and 8 capacitors C_{ij} in Figure 2(c) are reduced to 2 inductors and 2 capacitors in Figure 2(e). As a result, the undesired spurs disappear in our creation. The elements of C_{p1}, C_{p2}, L_{p1}, and L_{p2} in Figure 2(e) are easily evaluated by [5]

$$C_{p1} = C_{p2} = \sum_{i=1}^{7} C_{i,i+1} \tag{1}$$

$$L_{p1} = L_2||L_4||L_6||L_8 \tag{2}$$

$$L_{p2} = L_1||L_3||L_5||L_7 \tag{3}$$

Equations (1)–(3) illustrate the process of the parallel LC elements which are regrouped and merged, and the equivalent value of each element is shown in Figure 2(e). The capacitance can be calculated using S_{11} parameter by [2]

$$C = \frac{-1}{Z_0 2\pi f \mathrm{Im}\left(\dfrac{1+S_{11}}{1-S_{11}}\right)} \tag{4}$$

where f is the frequency, and Z_0 is the reference impedance.

3. SIMULATION AND MEASUREMENT

The proposed interdigital MIM capacitor is processed in a 2-layer LTCC material, whose single layer thickness is 0.1 mm, and dielectric constant is 5.9. Figure 3(a) shows the geometry configuration

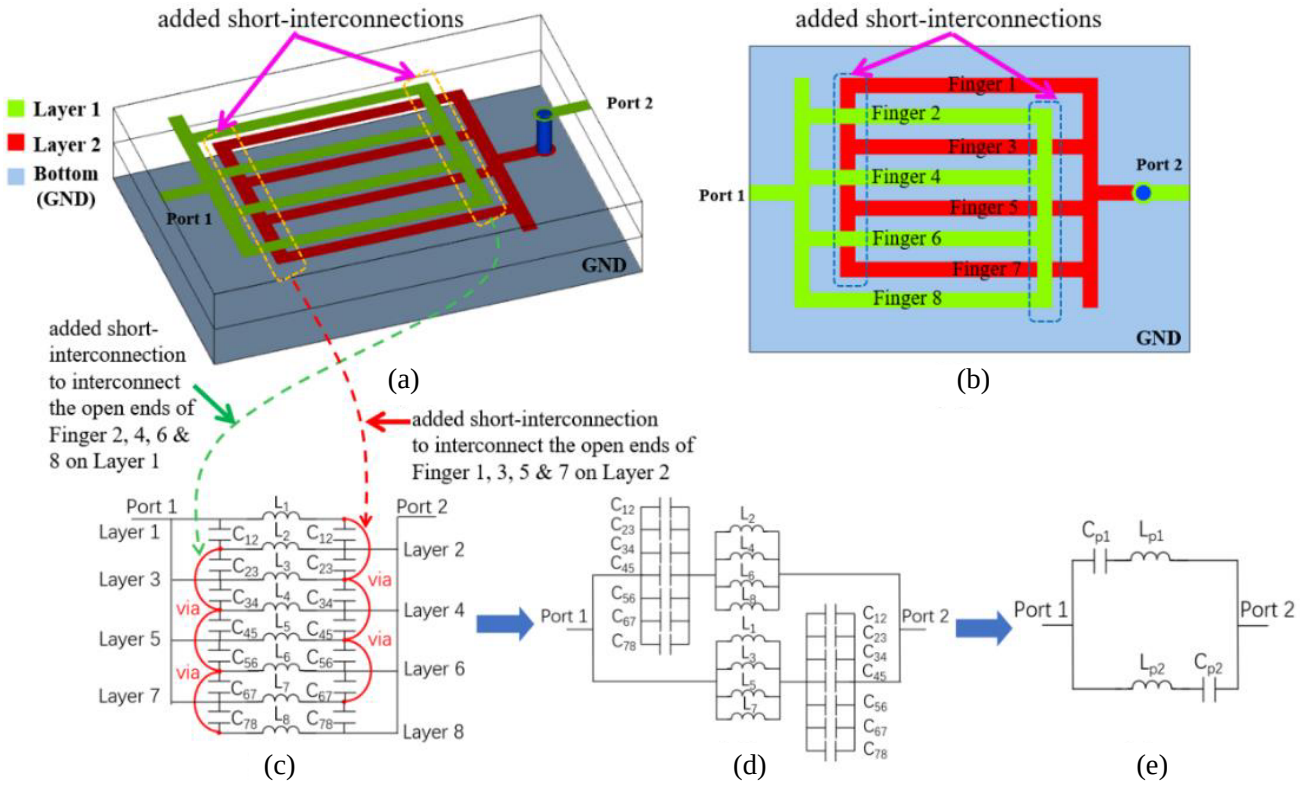

Figure 2. The proposed MIM capacitor, (a) 3D structure, (b) planar view, (c) equivalent circuit, (d) transformational circuit and (e) final circuit.

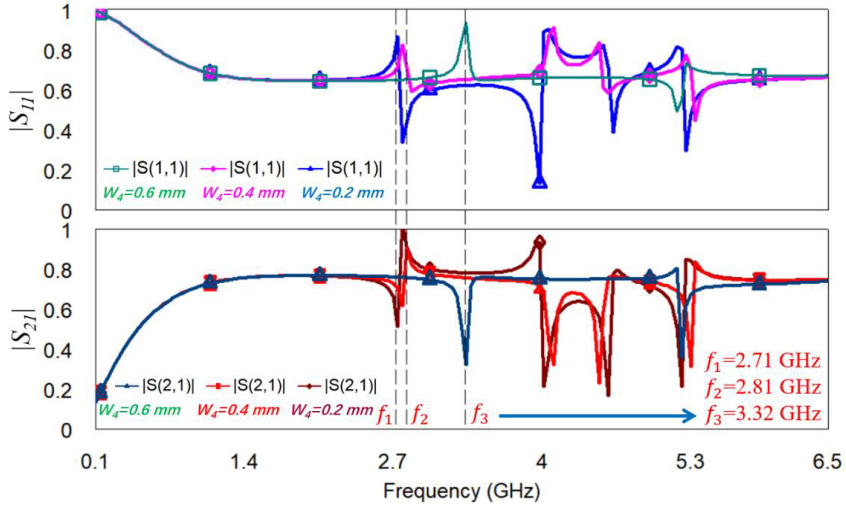

Figure 3. EM-simulated *s*-parameters with parameter variation.

with parameter definitions. To reach a capacitance higher than 13 pF from 0.1 to 7 GHz, parameters W_1, W_2, s, and *offset* are optimized with electromagnetic (EM) solver. As parameters W_1, W_2, s, and *offset* are calculated according to the required capacitance, the only parameter to optimize is W_4, which is the width of the added shorting interconnection. W_4 cannot be too wide nor too thin. Thin width of W_4 introduces inductance, which makes higher number of stopbands in its equivalent circuit or more spurs. On the other hand, wide width of W_4 results in series capacitance, which reduces its equivalent

Table 1. Dimensions of the proposed filters (unit: mm).

Parameter	W_0	W_1	W_2	W_3	W_4
Value	0.66	0.9	1.08	1.12	0.96
Parameter	L	s	r	R	*offset*
Value	7.2	2.26	0.66	1	2.1

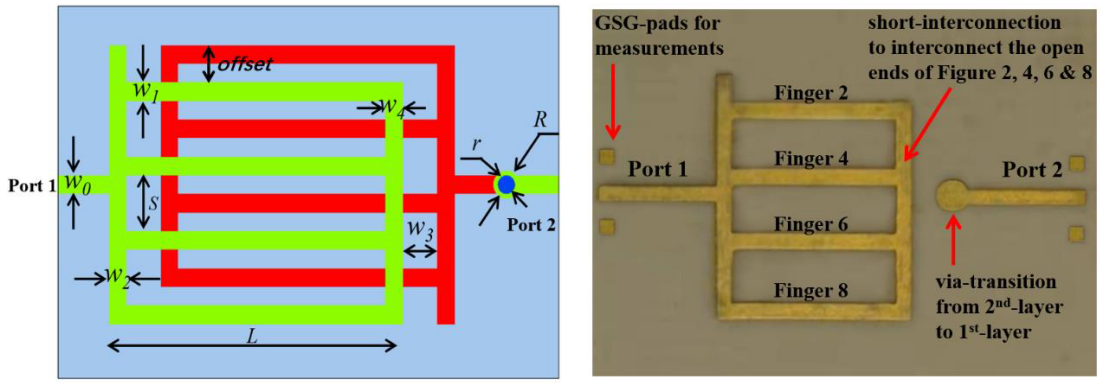

(a) (b)

Figure 4. (a) Geometry with parameters definitions and (b) photograph of the proposed interdigital MIM capacitor.

capacitance. Thus, the width W_4 of the added shorting interconnection has a strong influence of the proposed MIM. Parameter variation (W_4) has been implemented by EM-tool, and the s-parameters are shown in Figure 3. As can be seen in Figure 3, the 1st-spur occurs at f_1 (2.71 GHz), f_2 (2.82 GHz), and f_3 (3.32 GHz) when $W_4 = 0.2$ mm, $W_4 = 0.4$ mm, and $W_4 = 0.6$ mm, respectively. After a wider range of EM-optimization, the final EM-optimal parameters are listed in Table 1. A picture of the proposed creation is shown in Figure 4(b). Probe test station and Agilent N5230C network analyzer are used for our testing. Figure 6(a) shows the s-parameters of conventional and the proposed interdigital MIM capacitor after EM-simulations. Undesired spurs at f_1 (2.54 GHz), f_2 (3.14 GHz), f_3 (3.94 GHz), f_4 (4.42 GHz), and f_5 (5.06 GHz) disappear. We notice that the first spur's frequency is changed to f_T

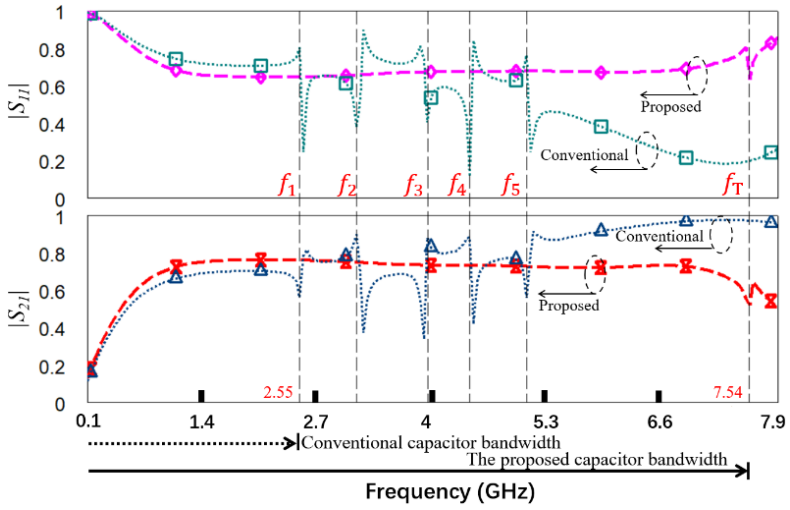

(a)

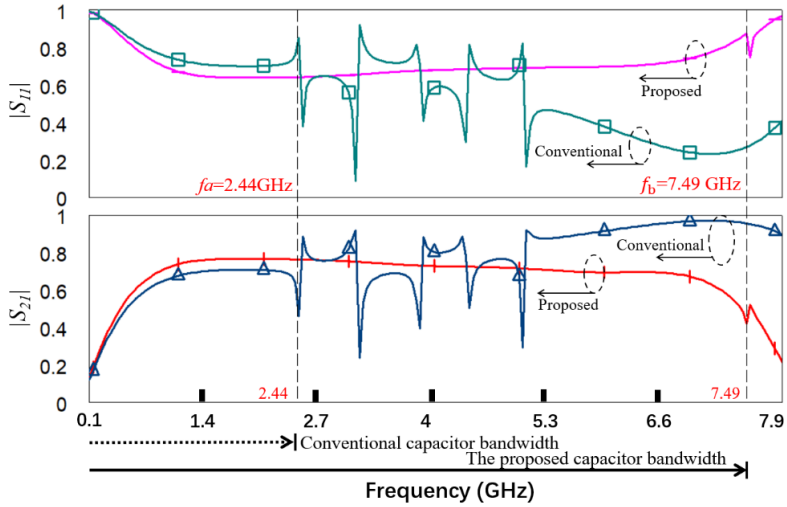

(b)

Figure 5. Results (a) EM-simulated s-parameters and (b) measured s-parameters.

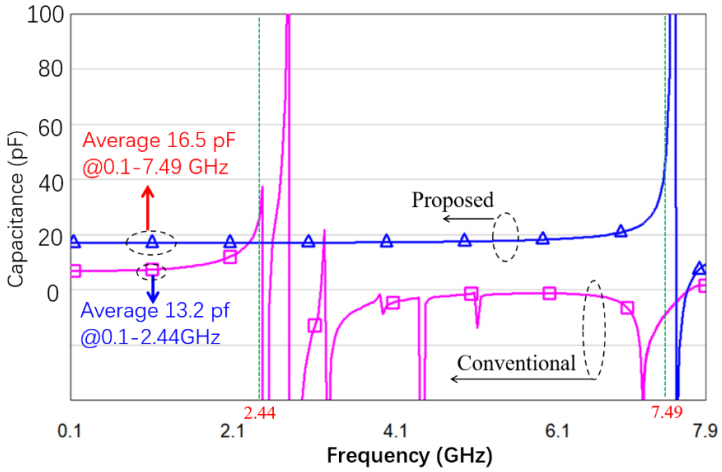

Figure 6. Capacitance extracted from the measured S_{11} parameters using Equation (4).

(7.54 GHz). Therefore, applicational frequency is expanded from 2.44 GHz to 7.49 GHz, which presents tremendous improvement. The first spur's frequency is conventional, and our creation after measuring is f_a (2.44 GHz) and f_b (7.49 GHz), respectively. Therefore, the practical bandwidth after measuring increases 206%, shown in Figure 5(b). The results between the simulation and measurement match well. The proposed capacitor has an average capacitance of 16.5 pF from 0.1 to 7.49 GHz (f_b), where as the average capacitance of conventional capacitor is only 13.2 pF from 0.1 to 2.44 GHz (f_a), shown in Figure 6. Thus, capacitance increases 25% compared with conventional implementation. The proposed interdigital capacitor has a wider frequency applicational range and a compact size of only 8.2×6.2 mm.

4. COMPARISON AND DISCUSSION

Comparison is also carried out between the proposed capacitor and other implementations [4–6], and the results are listed in Table 2. The proposed structure has the widest bandwidth and highest capacitance. The short-interconnecting method used to eliminate spurs here is much simpler than that in [3–6], because even-fingers on Layer 1 and odd-fingers on Layer 2 have no problem in interconnecting between

Table 2. Performance comparisons.

Ref.	Capacitor form	No. of fingers	Method	Frequency range extension (GHz)	Bandwidth increment (%)	Capacitance increment (%)	Fabrication process
[4]	Planar interdigital	8	Bond wires	$4.5 \rightarrow 7.5$	66	10	PCB
[5]	VIC	8	Vertically-interconnections	$3.4 \rightarrow 9.8$	188	8	LTCC
[6]	VIC	8	Vertically-interconnections	$4 \rightarrow 8$	100	20	LTCC
This work	Interdigital MIM	8	short-interconnections	$2.44 \rightarrow 7.49$	206	25	LTCC

interval fingers. In this creation, the series resonance does not restrict the bandwidth as the series resonance frequency is higher than the spur at f_5 in Figure 1. The proposed MIM has a wider frequency applicational range, which not only covers universal 2G/3G/4G/5G mobile communication applications, but also covers Band L, Band S, and Band C applications.

5. CONCLUSION

A wideband interdigital MIM capacitor is created and built with 206% bandwidth and 25% capacitance enhancement. Spur elimination is achieved with the reduction of stopband structures. Capacitance increment is reached without enlarging circuit size. The proposed interdigital capacitor has a wider frequency applicational range. Performance discussion and comparisons are also carried out.

REFERENCES

1. Chen, H.-Y., S.-S. Li, and M.-H. Li, "A low impedance CMOS-MEMS capacitive resonator based on metal-insulator-metal (MIM) capacitor structure," *IEEE Electron Device Letters*, Vol. 42, No. 7, 1045–1048, 2021.
2. Page, J. E., E. Marquez-Segura, F. P. Casares-Miranda, J. Esteban, P. Otero, and C. Camacho-Penalosa, "Exact analysis of the wire-bonded multiconductor transmission line," *IEEE Trans. Microw. Theory Tech.*, Vol. 88, No. 8, 1585–1592, 2007.
3. Zhou, B., C. Li, L. Qian, Y. Wang, and Z. Zhang, "Broadband vertically interdigital-capacitor with high frequency response improving," *Microwave and Optical Technology Letters*, Vol. 62, No. 12, 3779–3784, 2020.
4. Casares-Miranda, F. P., P. Otero, E. Marquez-Segura, and C. Camacho Penalosa, "Wire bonded interdigital capacitor," *IEEE Microw. Wirel. Compon. Lett.*, Vol. 15, No. 10, 700–702, 2005.
5. Bo, Z., W. Sheng, and Y. Zheng, "Miniaturized lumped-element LTCC filter with spurious spikes suppressed vertically-interdigital-capacitors," *IEEE Microw. Wirel. Compon. Lett.*, Vol. 24, No. 10, 692–694, 2014.
6. Zhou, B., L. Huang, Q. Chen, X. Ni, X. Li, N. Wang, and Z. Cai, "Wideband vertically-interdigital capacitor," *Proceedings of 2018 IEEE CPMT Symposium Japan (ICSJ)*, 201–204, Japan, 2018.